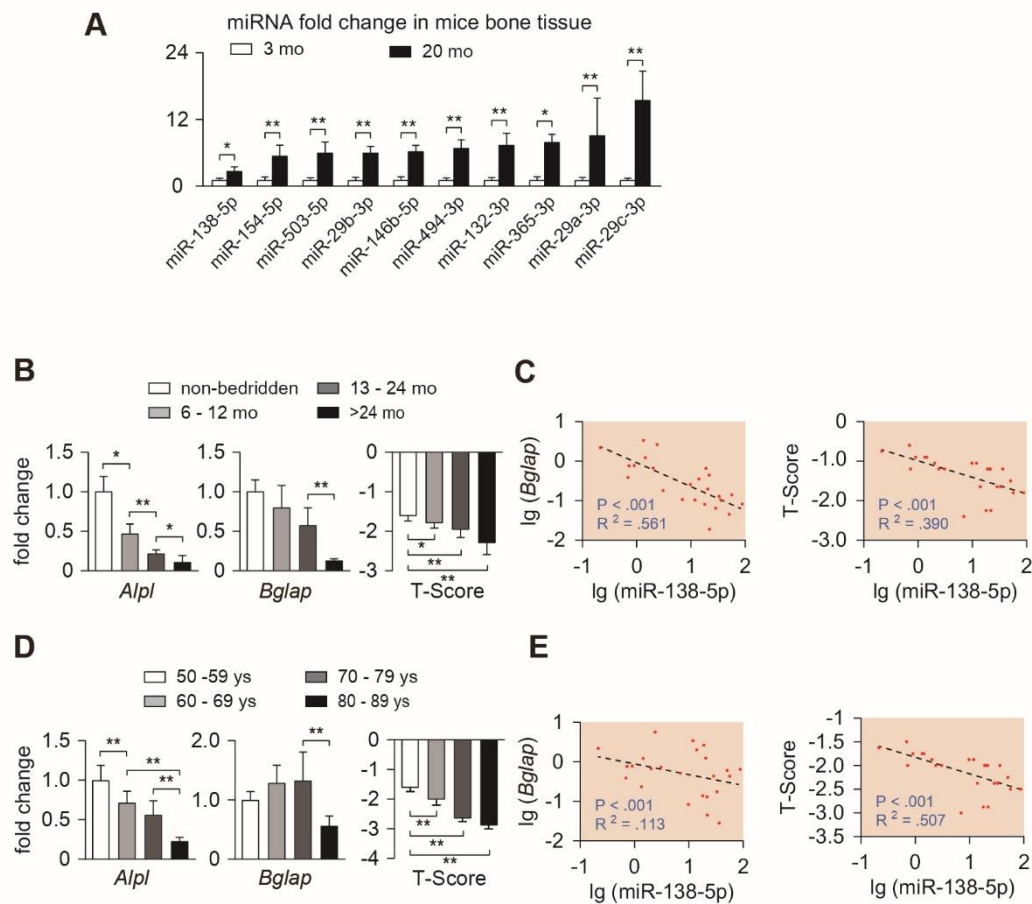
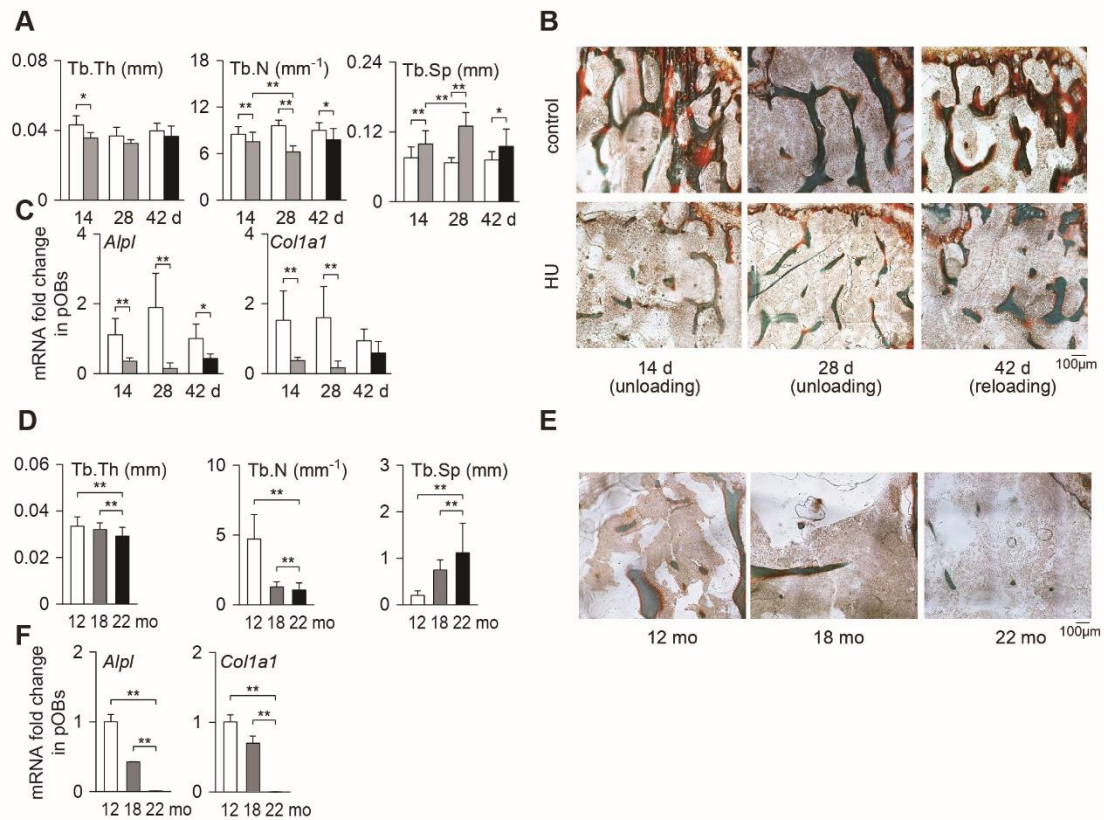


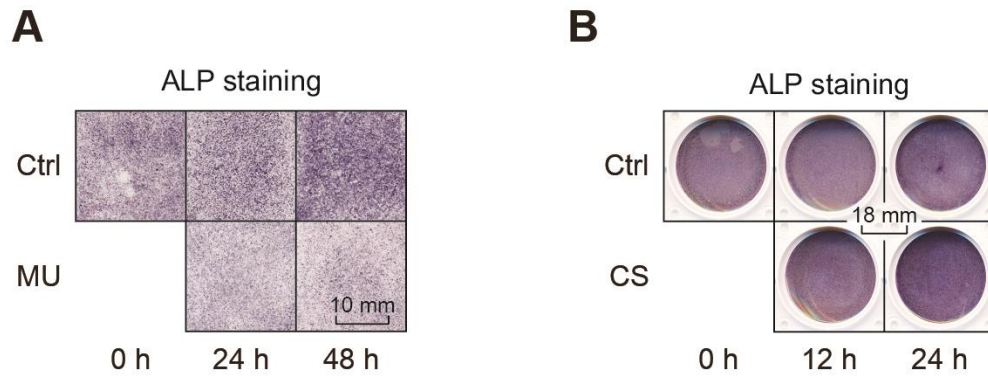
SUPPLEMENTARY FIGURES



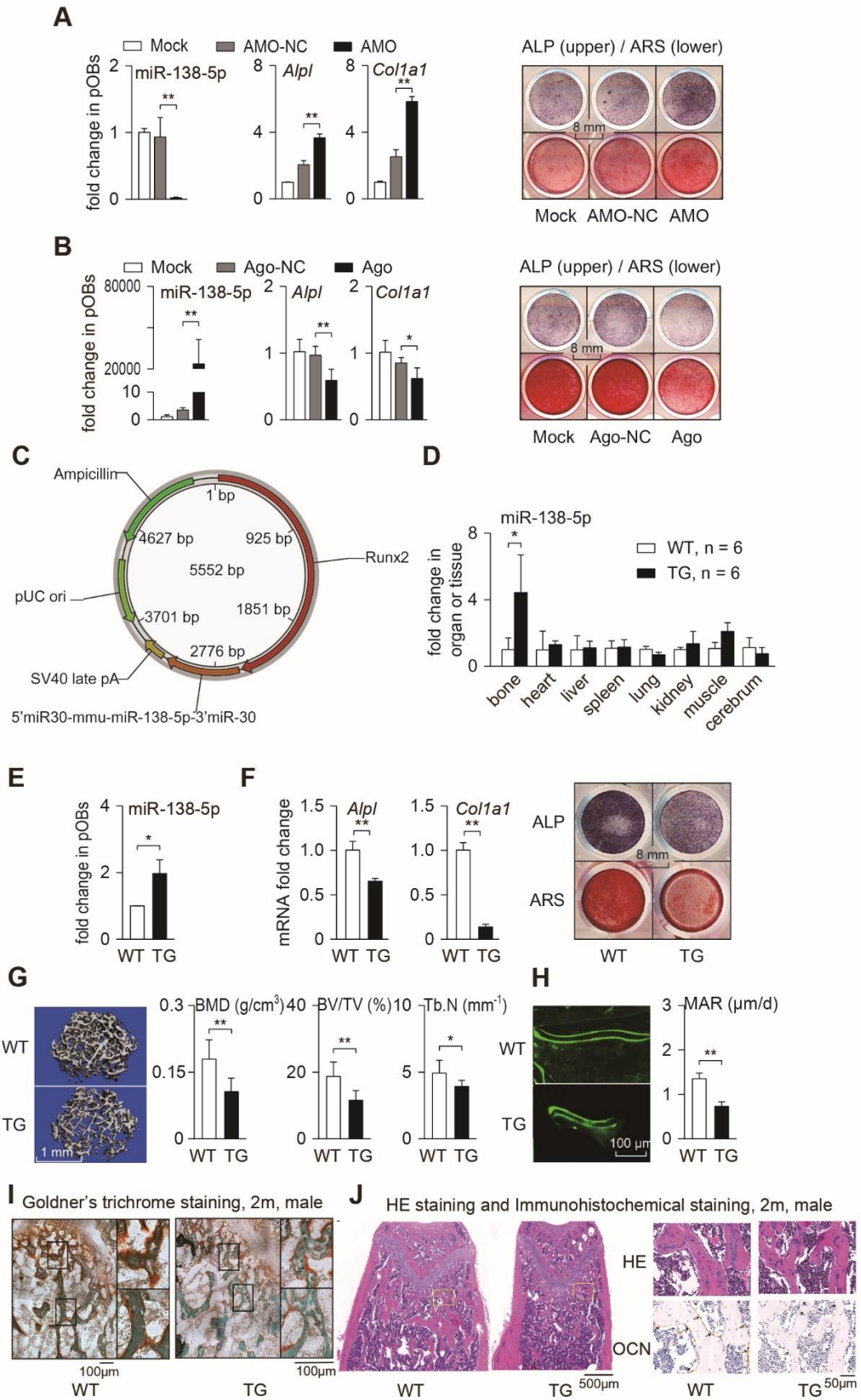
S-Figure 1. Changes of osteogenic marker genes and T-score in bedridden and aged osteoporotic patients. (A) Real-time PCR analysis of candidate mechanosensitive miRNAs levels in bone tissues of 3-month-old and 20-month-old mice. $n = 4$ in each group. (B) Real-time PCR analysis of *Alpl* (left) and *Bglap* (middle) levels in bone specimens and T-score (right) of femoral neck from bedridden men patients (50-59 years old) with different periods of immobilization. $n = 6$ in each group. (C) Linear regression analysis of miR-138-5p and *Bglap* (left) and T-score (right) association in bone specimens from bedridden men patients (50-59 years old) with different periods of immobilization. (D) Real-time PCR analysis of *Alpl* (left) and *Bglap* (middle) levels in bone specimens and T-score (right) of femoral neck from aged men patients (non-bedridden). $n = 6$ in each group. (E) Linear regression analysis of miR-138-5p and *Bglap* (left) and T-score (right) association in bone specimens from aged men patients (non-bedridden). *Gapdh* was used as the internal control for mRNAs. Data are represented as mean \pm sem. Significances were determined using student's *t*-test between two groups. P value less than 0.05 were considered significant in all cases (* $P < 0.05$, ** $P < 0.01$).



S-Figure 2. Analysis of bone formation in reloaded mice and aged mice. (A) MicroCT statistical analysis of trabecular thickness (Tb.Th), trabecular number (Tb.N), trabecular spacing (Tb.Sp), in distal femur of hindlimb unloaded or reloaded mice. $n \geq 6$ for each group. (B) Representative images of osteoid formation indicated by Goldner's trichrome staining in distal femur of hindlimb unloaded or reloaded mice. Scale bar, 100 μm . (C) Real-time PCR analysis of *Alpl* and *Col1a1* mRNA levels in primary osteoblasts isolated from hindlimb unloaded and reloaded mice, respectively. $n = 6$ for each group. (D) MicroCT statistical analysis of trabecular thickness (Tb.Th), trabecular number (Tb.N), trabecular spacing (Tb.Sp), in distal femur of 12, 18 and 22-month-old male C57BL/6 mice. $n = 6$ for each group. (E) Representative images of osteoid formation indicated by Goldner's trichrome staining in distal femur of 12, 18 and 22-month-old male C57BL/6 mice. Scale bar, 100 μm . (F) Real-time PCR analysis of *Alpl* and *Col1a1* mRNA levels in primary osteoblasts from 12, 18 and 22-month-old male C57BL/6 mice, respectively. $n = 3$ for each group. *Gapdh* was used as the internal control for mRNAs. Data are represented as mean \pm s.d. Significances were determined using student's *t*-test between two groups. *P* value less than 0.05 was considered significant in all cases (* $P < 0.05$, ** $P < 0.01$).



S-Figure 3. Time-course changes of ALP activity in primary osteoblasts under mechanical unloading or cyclic stretch. (A) Representative images of ALP staining in primary osteoblasts cultured for 0, 24, and 48 h under mechanical unloading (MU), respectively. Scale bar, 10 mm. (B) Representative images of ALP staining in primary osteoblasts cultured for 0, 12, and 24 h under cyclic stretch (CS), respectively. Scale bar, 18 mm.

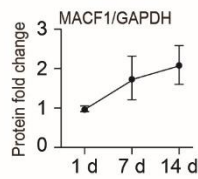
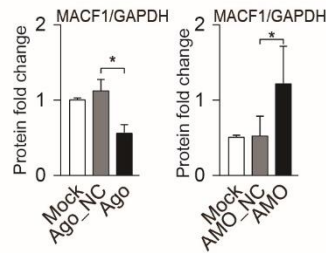
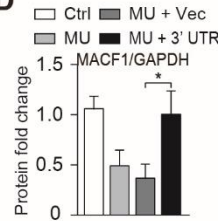
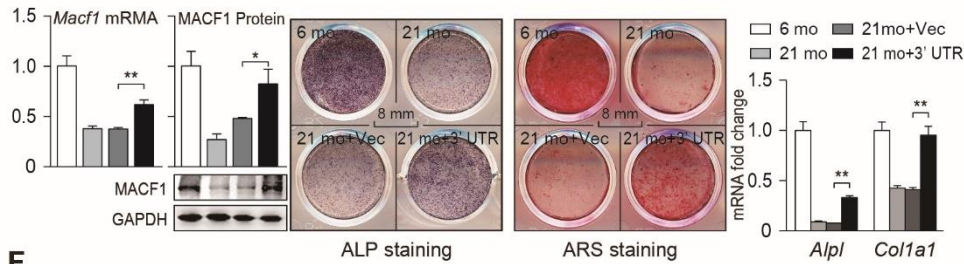
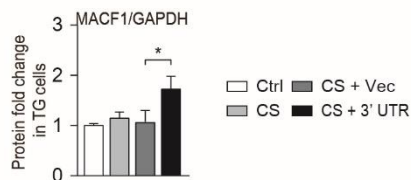


S-Figure 4. miR-138-5p negatively regulates osteoblast differentiation and bone formation.

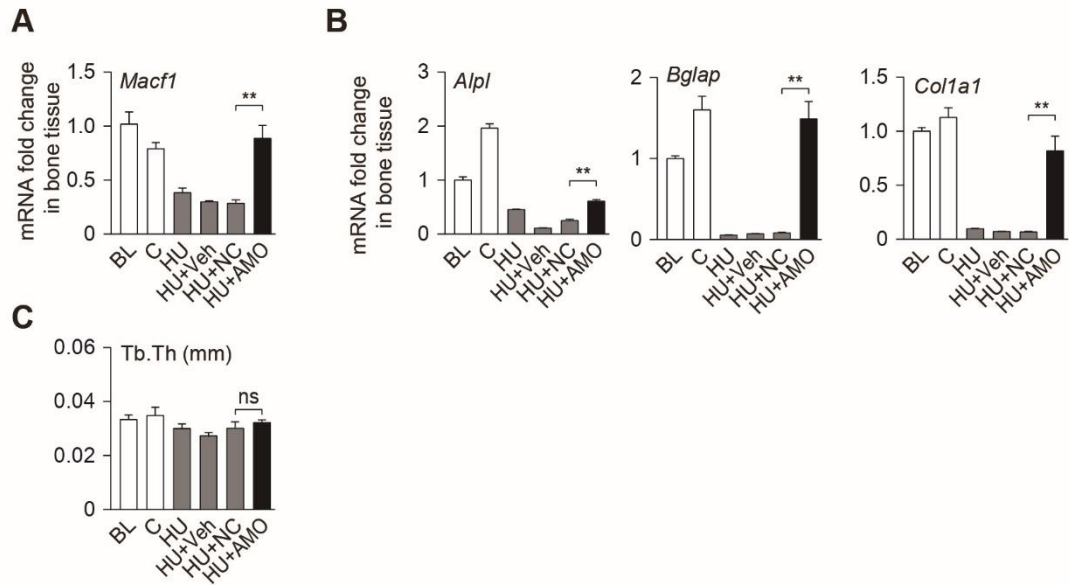
(A) Real-time PCR analysis of miR-138-5p (left) and osteogenic marker genes *Alpl* and *Colla1* mRNA levels (middle), and representative images of ALP staining (right, upper) and Alizarin Red S (ARS) staining (right, lower, 10 d) in primary osteoblasts treated with miR-138-5p antagonist (AMO). Scale bar, 8 mm. (B) Real-time PCR analysis of miR-138-5p (left) and osteogenic marker genes *Alpl* and *Colla1* mRNA levels (middle), and representative images of ALP staining (right, upper) and ARS staining (right, lower, 14 d) in primary osteoblasts treated with miR-138-5p agonist (Ago). Scale bar, 8 mm. (C) The Recombinant (pRP (Exp)-RUNX2>5'miR30-mmu-miR-138-5p-3'miR30) plasmid was constructed with the Runx2 promoter. (D) Real-time PCR analysis of miR-138-5p level in organs or tissues from 2-month male wild type (WT) and osteoblastic miR-138-5p transgenic (TG) mice. (E) Real-time PCR analysis of miR-138-5p level in primary osteoblasts isolated from 2-month male WT and TG mice. (F) Real-time PCR analysis of *Alpl* and *Colla1* mRNA levels (left), and representative images of ALP staining (right, upper) and ARS staining (right, lower, 14 d) in primary osteoblasts isolated from 2-month male WT and TG mice. Scale bar, 8 mm. (G) Representative 3D reconstruction images showing microarchitecture (left), and microCT statistical analysis of BMD, BV/TV, Tb.N (right) in distal femur of 2-month male WT and TG mice. BMD, bone mineral density; BV/TV, bone volume fraction; Tb.N, trabecular number. Scale bar, 1 mm. (H) Representative calcein double labeling images (left) and dynamic histomorphometric analysis of MAR (right) showing bone formation capacity in distal femur of 2-month male WT and TG mice. Scale bar, 100 μ m. (I) Representative images of osteoid formation indicated by Goldner's trichrome staining in distal femur of 2-month male WT and TG mice. Scale bar, 100 μ m. (J) Representative images of H&E staining and immunohistochemical staining analysis of osteocalcin (OCN) in distal femur of 2-month male WT and TG mice. Scale bar, 500 μ m and 50 μ m. U6 small nuclear RNA was used as the internal control for miR-138-5p, and *Gapdh* was used as the internal control for mRNAs. For mice, $n \geq 6$ in each group. For cell experiments, $n = 3$ in each group for Real-time PCR analysis. Data are represented as mean \pm s.d. Significances were determined using student's *t*-test between two groups. *P* value less than 0.05 was considered significant in all cases (**P* < 0.05, ***P* < 0.01).

A

	predicted consequential pairing of target region (top) and miRNA (bottom)	Site type	Context++ score	Context++ score %	Weighted context++ score	Conserved branch length	P_{CT}
<i>Macf1</i> 3' UTR 5' ... UCCUUUAACGGAGUU	921 ACCAGCA 928 mmu-miR-138-5p 3' GCCGGACUAAGUGUU JGGUCCA	8mer	-0.49	97	-0.45	4.375	0.87
<i>MACF1</i> 3' UTR 5' ... UCCUUUA AUGGAGUU	943 ACCAGCA 950 hsa-miR-138-5p 3' GCCGGACUAAGUGUU JGGUCCA	8mer	-0.52	98	-0.48	4.375	0.87

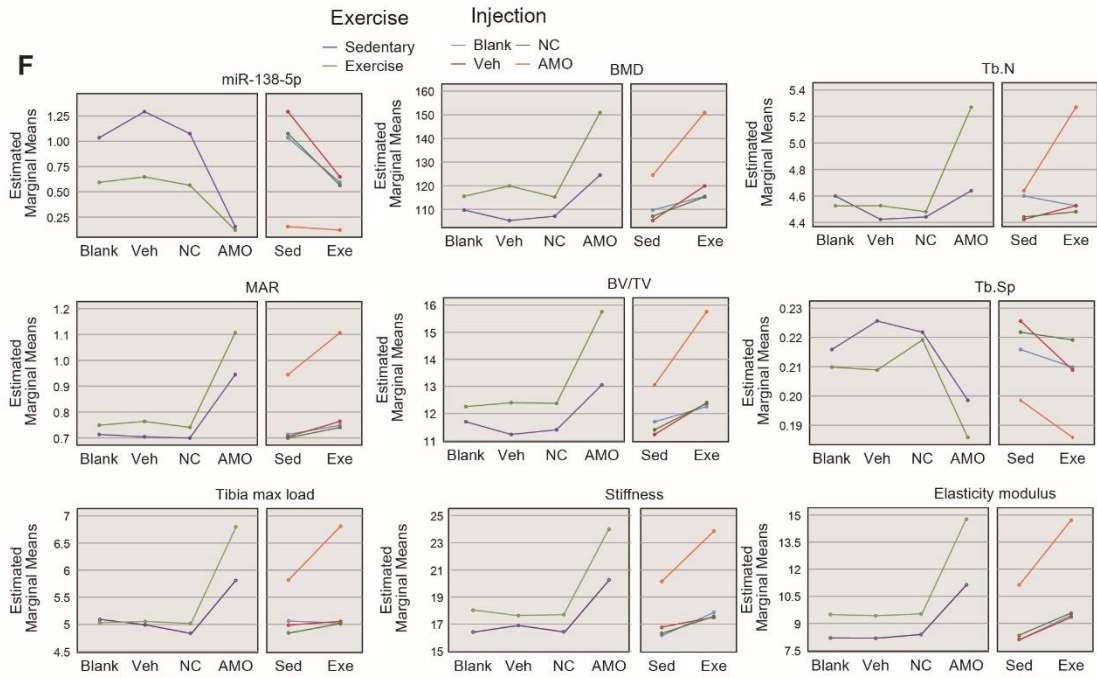
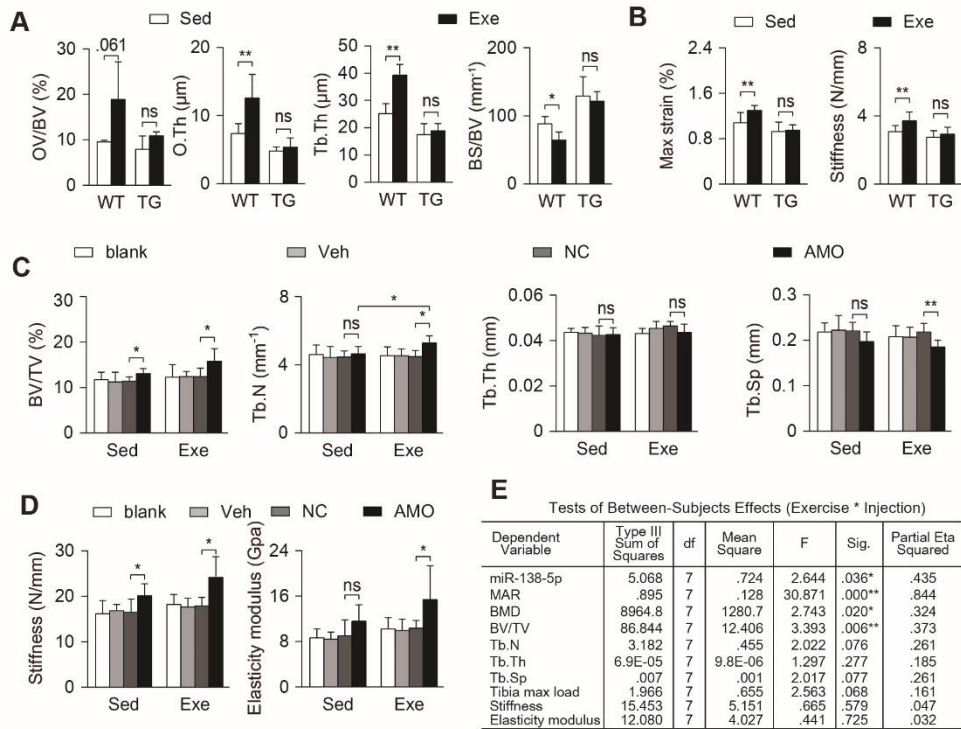
B**C****D****E****F**

S-Figure 5. miR-138-5p targets MACF1 to inhibit aged osteoblast differentiation. (A) Sequence alignments between miR-138-5p and candidate binding sites in the *Macf1* 3' UTR predicted with the TargetScan database. (B) Quantification of MACF1 protein level in primary osteoblasts during osteo-induction. (C) Quantification of MACF1 protein level in primary osteoblasts treated with either miR-138-5p agonist (Ago) or antagonist (AMO), respectively. (D) Quantification of MACF1 protein level in primary osteoblasts treated with *Macf1* 3'UTR plasmid or blank vector under MU condition, respectively. (E) Real-time PCR and western blot (left) analysis of MACF1 levels, representative images of ALP staining (middle, left) and ARS staining (middle, right, 16 d), and Real-time PCR analysis of *Alpl* and *Col1a1* mRNA levels (right) in primary 21-month aged osteoblasts treated with *Macf1* 3'UTR plasmid or blank vector. Scale bar, 8 mm. (F) Quantification of MACF1 level in TG cells treated with *Macf1* 3' UTR plasmid or blank vector under CS condition, respectively. *Gapdh* was used as the internal control for mRNAs. $n = 3$ in each group for Real-time PCR and Western Blot analysis. Data are represented as mean \pm s.d. Significances were determined using student's *t*-test between two groups. *P* value less than 0.05 were considered significant in all cases (* $P < 0.05$, ** $P < 0.01$).

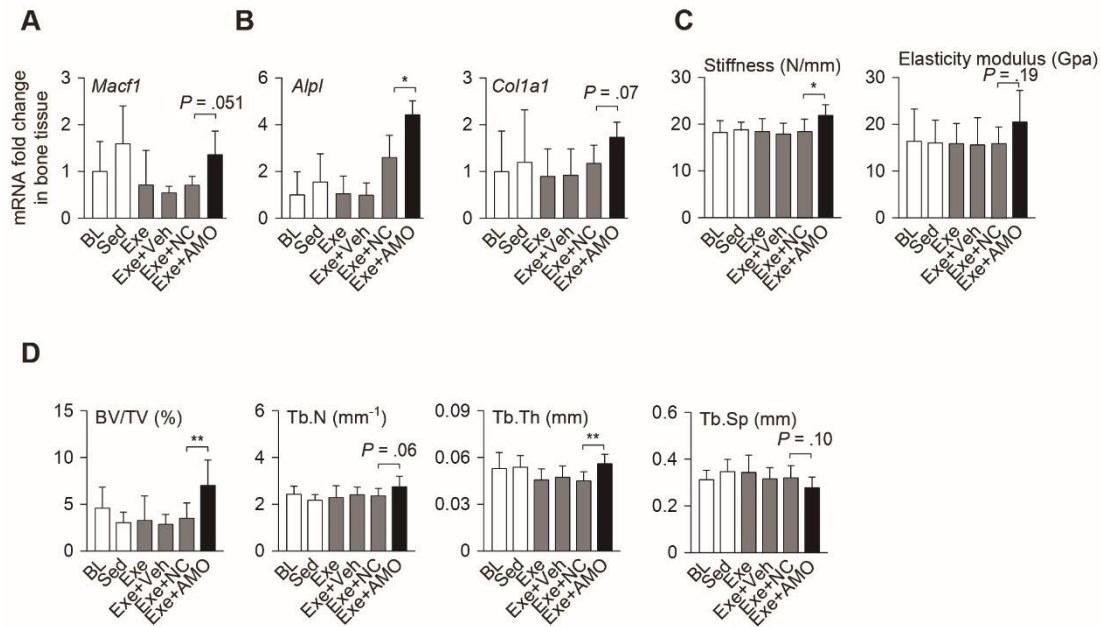


S-Figure 6. miR-138-5p antagonist restores unloading-induced decrease of bone formation.

(A) Real-time PCR analysis of *Macf1* mRNA levels in bone tissue of all groups. $n = 4$ in each group. BL (baseline, 3-month-old mice), C (4-month-old mice, without any injection), HU (4-month-old mice, hindlimb unloading for 28d without any injection), HU + Veh (4-month-old mice, hindlimb unloading for 28d and injected with osteoblast-targeted delivery system), HU + NC (4-month-old mice, hindlimb unloading for 28d and injected with both osteoblast-targeted delivery system and antagomir-NC), HU + AMO (4-month-old mice, hindlimb unloading for 28d and injected with both osteoblast-targeted delivery system and antagomir-138-5p). (B) Real-time PCR analysis of *Alpl*, *Col1a1* and *Bglap* mRNA levels in bone tissue of all groups. $n = 4$ in each group. (C) microCT statistical analysis of trabecular thickness (Tb.Th) in distal femur of hindlimb unloaded mice pretreated with AMO. $n \geq 5$ mice for each group. *Gapdh* was used as the internal control for mRNA. Data are represented as mean \pm s.d. Significances were determined using student's *t*-test between two groups. *P* value less than 0.05 was considered significant in all cases (** $P < 0.01$).



S-Figure 7. miR-138-5p overexpression loses mechano-sensitization of anabolic bone action in miR-138-5p transgenic osteoporotic mice. (A) Statistical analysis of osteoid parameters (OV/BV and O.Th) and trabecular parameters (Tb.Th and BS/BV) in distal femur of miR-138-5p transgenic (TG) mice and wild type (WT) mice after 4-week treadmill exercise. Sed, sedentary, Exe, exercise. $n = 4$ mice for each group. OV/BV: osteoid volume per bone volume; O.Th: osteoid thickness; Tb.Th: trabecular thickness; BS/BV: Bone surface per bone volume. (B) Three-point bending measurement of femur maximum strain and stiffness in femur of WT and TG mice after treadmill exercise. $n \geq 5$ mice for each group. (C) MicroCT analysis of BV/TV, Tb.N, Tb.Th, Tb.Sp in distal femur after treadmill exercise and AMO treatment. $n = 6$ for each group. BV/TV, bone volume fraction; Tb.N, trabecular number; Tb.Th, trabecular thickness; Tb.Sp, trabecular spacing. Blank (without any injection), Veh (injected with osteoblast-targeted delivery system), NC (injected with both osteoblast-targeted delivery system and antagomir-NC), AMO (injected with both osteoblast-targeted delivery system and antagomir-138-5p). Sed, sedentary, Exe, exercise. (D) Three-point bending measurement of tibia stiffness and elasticity modulus in femur after treadmill exercise and AMO treatment. $n = 6$ for each group. Data are represented as mean \pm s.d. Significances were determined using student's *t*-test between two groups. *P* value less than 0.05 was considered significant in all cases (ns, no difference, $*P < 0.05$, $**P < 0.01$). (E) Tests of Between-subjects Effects (Exercise and injection) of miR-138-5p, MAR, BMD, BV/TV, Tb.N, Tb.Th, Tb.Sp, tibia max load, stiffness and elasticity modulus in all groups. (F) Two-way ANOVA analysis of Estimated Marginal Means of miR-138-5p, MAR, BMD, BV/TV, Tb.N, Tb.Sp, tibia max load, stiffness and elasticity modulus in all groups.



S-Figure 8. miR-138-5p antagonist sensitizes anabolic bone action to mechanical stimuli in aged osteoporotic mice. (A) Real-time PCR analysis of *Macf1* mRNA level in bone tissue of all groups. *n* = 4 in each group. BL (baseline, 20-month-old mice), Sed (21-month-old mice, without any injection and without treadmill), Exe (21-month-old mice, treatment with treadmill exercise and without any injection), Exe + Veh (21-month-old mice, treatment with treadmill exercise and injected with osteoblast-targeted delivery system), Exe + NC (21-month-old mice, treatment with treadmill exercise and injected with osteoblast-targeted delivery system and antagomir-NC), Exe + AMO (21-month-old mice, treatment with treadmill exercise and injected with osteoblast-targeted delivery system and antagomir-138-5p). (B) Real-time PCR analysis of *Alpl* and *Col1a1* mRNA levels in bone tissue of all groups. *n* = 4 in each group. (C) Three-point bending measurement of tibia stiffness and elasticity modulus in femur of all groups. *n* ≥ 5 mice for each group. (D) MicroCT analysis of BV/TV, Tb.N, Tb.Th, Tb.Sp in distal femur after treadmill exercise and AMO treatment. *n* ≥ 5 mice for each group. BV/TV, bone volume fraction; Tb.N, trabecular number; Tb.Th, trabecular thickness; Tb.Sp, trabecular spacing. *Gapdh* was used as the internal control for mRNA. Data are represented as mean ± s.d. Significances were determined using student's *t*-test between two groups. *P* value less than 0.05 was considered significant in all cases (**P* < 0.05, ***P* < 0.01).

S-Table 1 Clinical features of patients involved in bone specimens analysis

Patient	Age	Gender	Bedridden time (months)	T-score for femoral neck
1	55	Male	NA	-1.6
2	57	Male	NA	-1.8
3	54	Male	NA	-1.5
4	52	Male	NA	-1.7
5	58	Male	NA	-1.4
6	59	Male	NA	-1.6
7	54	Male	6	-1.8
8	57	Male	8	-1.8
9	55	Male	9	-1.7
10	51	Male	7	-1.6
11	59	Male	10	-1.8
12	54	Male	11	-2
13	53	Male	14	-2.2
14	55	Male	16	-1.8
15	56	Male	15	-1.7
16	57	Male	18	-1.8
17	54	Male	20	-2.1
18	58	Male	21	-2.1
19	53	Male	25	-1.8
20	52	Male	26	-2.5
21	54	Male	26	-2.2
22	56	Male	27	-2.6
23	56	Male	25	-2.1
24	57	Male	28	-2.5
25	67	Male	NA	-1.9
26	63	Male	NA	-2.1
27	62	Male	NA	-1.8
28	68	Male	NA	-2.3
29	66	Male	NA	-2.8
30	68	Male	NA	-2.1
31	76	Male	NA	-2.6
32	72	Male	NA	-2.5
33	77	Male	NA	-2.7
34	76	Male	NA	-2.5
35	76	Male	NA	-2.7
36	78	Male	NA	-2.8
37	88	Male	NA	-3.1
38	86	Male	NA	-2.9
39	84	Male	NA	-2.8
40	83	Male	NA	-2.7
41	84	Male	NA	-2.8
42	88	Male	NA	-2.9

